

Atomistic simulation studies of the α/β -glucoside and galactoside in anhydrous bilayers: effect of the anomeric and epimeric configurations

Sara Ahmadi · Vijayan Manickam Achari ·
HockSeng Nguan · Rauzah Hashim

Received: 18 September 2013 / Accepted: 31 January 2014 / Published online: 13 March 2014
© Springer-Verlag Berlin Heidelberg 2014

Abstract Fully atomistic molecular dynamics simulation studies of thermotropic bilayers were performed using a set of glycosides namely n-octyl- β -D-glucopyranoside (β -C8Glc), n-octyl- α -D-glucopyranoside (α -C8Glc), n-octyl- β -D-galactopyranoside (β -C8Gal), and n-octyl- α -D-galactopyranoside (α -C8Gal) to investigate the stereochemical relationship of the epimeric/anomeric quartet liner glycolipids with the same octyl chain group. The results showed that, the anomeric stereochemistry or the axial/equatorial orientation of C1–O1 (α/β) is an important factor controlling the area and *d*-spacing of glycolipid bilayer systems in the thermotropic phase. The head group tilt angle and the chain ordering properties are affected by the anomeric effect. In addition, the L_C phase of β -C8Gal, is tilting less compared to those in the fluid L _{α} . The stereochemistry of the C4-epimeric (axial/equatorial) and anomeric (α/β) centers simultaneously influence the inter-molecular hydrogen bond. Thus, the trend in the values of the hydrogen bond for these glycosides is β -C8Gal > α -C8Glc > β -C8Glc > α -C8Gal. The four bilayer systems showed anomalous diffusion behavior with an observed trend for the diffusion coefficients; and this trend is β -C8Gal > β -C8Glc > α -C8Gal > α -C8Glc. The “bent” configuration of the α -anomer results in an increase of the hydrophobic area, chain vibration and chain disorganization. Since

thermal energy is dispensed more entropically for the chain region, the overall molecular diffusion decreases.

Keywords Molecular dynamics simulation · Glycolipid · Anomalous diffusion · Sugar stereochemistry

Introduction

Sugar has intriguing structural diversity that gives rise to complex behavior. Even in the simplest monosaccharide, i.e., a single sugar unit, the diverse possible stereochemical arrangement of the hydroxyl groups gives rise to different types of sugars, like glucose, mannose, and galactose. The last two are glucose epimers, where the hydroxyl group at the 2 and 4 carbon positions within the sugar ring is axially oriented for mannose and galactose respectively, instead of equatorial as in the case of glucose (Fig. 1). The complexity increases further when these sugar units combine to form disaccharides, oligomers and polymers or when they combine with other conjugates like proteins to form glycoproteins and lipids to form glycolipids (GLs). The precise effect of sugar stereochemistry is very much guesswork, but how this affects the macroscopic behavior is very profound, for example, while starch and cellulose are very different materials, their microscopic components are related very closely. Maltose differs from cellobiose only at the 1–4 link between the two sugar units [1]. Similarly glucolipid and galactolipid behave differently in self-assembly and biomembrane [2] but glucose and galactose are only slightly different (see Fig. 1). The functional differentiation due to sugar stereochemistry may be further exemplified by the observation that galactose-based glycolipids (GLs) are commonly found in plant membranes, while glucose-based kinds are usually associated with microorganisms [3].

Electronic supplementary material The online version of this article (doi:10.1007/s00894-014-2165-0) contains supplementary material, which is available to authorized users.

S. Ahmadi · V. Manickam Achari · H. Nguan · R. Hashim (✉)
Chemistry Department, faculty of Science, University of Malaya,
Kuala Lumpur 50603, Malaysia
e-mail: rauzah@um.edu.my

S. Ahmadi
Kavli Institute for Theoretical Physics, Chinese Academy of
Sciences, Beijing 100190, China

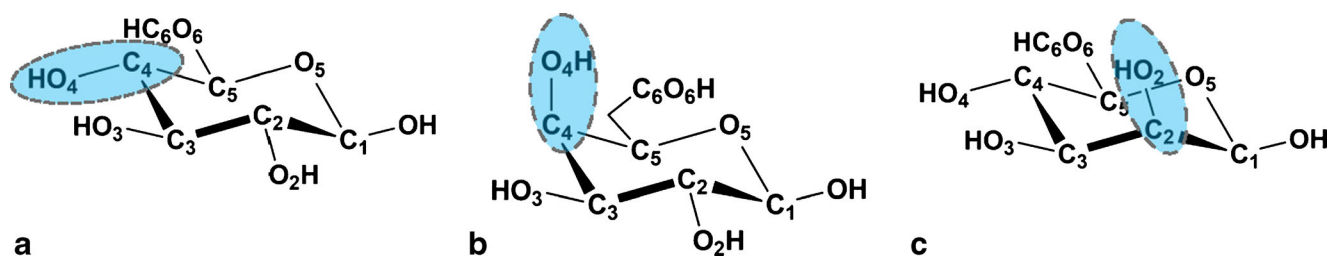


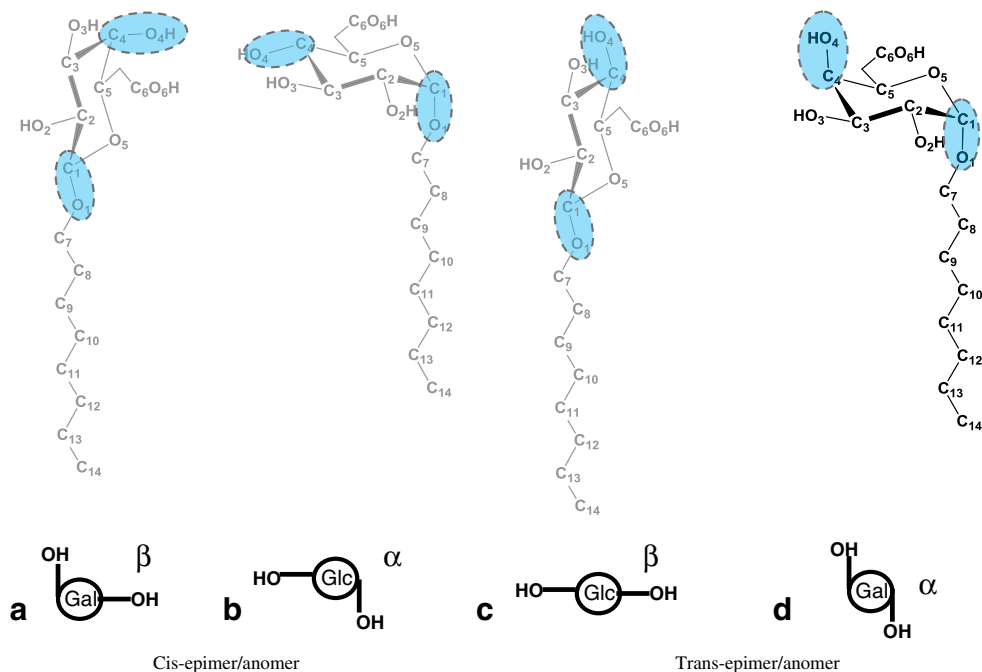
Fig. 1 Chemical structures for (a) glucose, (b) mannose, and (c) galactose

Even though GLs are commonly associated with biological membrane, their amphiphilic nature, i.e., possessing both a water-loving hydrophilic sugar headgroup and water-hating hydrophobic alkyl chain, means GLs may self-assemble into a variety of liquid crystal phases, e.g., lamellar and hexagonal, in dry (thermotropic) as well as in solvent (lyotropic) [4]. Therefore, these amphitropic materials [5] have a wider application potential not confined to those related to the lyotropic phases (e.g., surfactants and delivery systems [6]), but possibly also those derived from the dry thermotropic phase. Novel thermotropic applications of GLs have yet to be developed and realized. Unfortunately, due to lack of interest (or possibly awareness) not many fundamental studies have been carried out in the GLs thermotropic phase to support application development. However, recently some of these application related studies were reported, for example taking advantage of the sugar headgroup being chiral and tilted structures (i.e., S_C) in the lipid organization which imply possible ferroelectric behavior (see for example [2] and references therein). Thus, in the present study, we focus on the thermotropic phase of these GLs, in particular a set of four alkyl glycosides related epimerically (gluco- versus galacto-)

and anomerically (α - and β -) to understand how these stereochemical factors, which give rise to different hydrogen bonding networks in the hydrophilic region govern the anhydrous self-assembly properties, and in turn are related to their liquid crystal clearing transition temperatures.

These glycosides, have been widely studied fundamentally in the lyotropic phase [7] as well as for applications, e.g., in membrane protein crystallization [8]. The structural difference between, α -C8Glc and β -C8Glc, is only at the anomeric C1 position (Fig. 2), where the glycosidic bond points axially for the former and equatorially for the latter. This subtle variation in molecular orientation gives a large difference in the phase diagrams of β -C8Glc and α -C8Glc [7]. In addition, as demonstrated by a simulation study of these compounds, the solvent-accessible surface area, head group cluster structure, and the number of isolated water molecules show significant changes despite properties like shape and surfactant chain length remaining the same [9]. The anomeric effect on the self-assembly behavior of linear alkyl glycosides has been well documented [10, 11]. Recently, Hashim et al., [10] observed a general trend in the thermotropic clearing points for a set of four glycolipids which are epimerically and

Fig. 2 Chemical structures for glycolipids, (a) *n*-octyl- β -D-galactopyranoside (β -C8Gal), (b) *n*-octyl- α -D-gluco-pyranoside (α -C8Glc), (c) *n*-octyl- β -D-gluco-pyranoside (β -C8Glc), and (d) *n*-octyl- α -D-galactopyranoside (α -C8Gal)



anomerically related α/β -C8Gal and α/β -C8Glc. The thermotropic clearing transition temperatures of these glycolipids are in the order of $T_{\beta\text{Gal}} > T_{\alpha\text{Glc}} > T_{\beta\text{Glc}} \sim T_{\alpha\text{Gal}}$. The trend seems to apply for GLs with different chain lengths as well as branched chains. This has led to speculation that the epimeric/anomeric pairs may have similar structural arrangements (hence interaction) within their hydrophilic region. The present objective is to find molecular substantiation using computer simulation on the likely relationship between two pairs of liner glycolipids, namely, α/β -octyl-galactosides (α/β -C8Gal) and α/β -octyl-glucosides (α/β -C8Glc) by modeling its thermotropic smectic A (or L_α the equivalent phase nomenclature proposed by Luzzati [12]) close to the liquid crystal clearing phase transition temperature. In this manuscript, we used the latter nomenclature for these bilayer systems, while the naming convention of the molecules is given in Fig. 2. A similar study on a set of double bilayer systems namely α/β -C8Gal and α/β -Glc was previously conducted by Chong et al. [13]. However, it differs in many ways from the current study. The former simulation was performed in the L_C (i.e., lamellar crystal phase at 27 °C), while the current study chose a temperature of 90 °C and focuses on mainly the L_{α} , which is known to be stable at a much higher temperature according to the phase diagram [7]. Thus, the current simulation results compare directly to the experimentally observed liquid crystal phase of these materials. The present simulation methodology, which employs a single bilayer allows for a much longer simulation time of 200 ns as compared to the previous 5 ns simulation [13]. A long simulation is necessary to calculate basic equilibrium properties, such as the area per lipid [14]. In addition, many interesting events, including diffusion in solids and chemical reactions, which are called “infrequent” or “rare” events occur at a longer time scale [15]. In the present simulation study, the area per lipid requires on average 30 to 40 ns to reach equilibrium. The slow convergence of this property proves that the generation of sufficient equilibrium samples cannot be acquired in a few nanoseconds simulations. Therefore, the results presented here are more reliable. Consequently, we have computed some dynamical properties not analyzed previously.

The four bilayer systems were simulated at 90 °C. According to the phase diagram, at 90 °C β -C8Glc [7] and α -C8Glc [16] are in the L_α phase. However, there is no phase diagram available for α -C8Gal, but Hashim et al. [10] reported this compound exists in the L_α phase within the temperature range between 40–98 °C. On the other hand, at 90 °C, β -C8Gal [7] is in the L_C phase but close to the phase boundary of L_α . Unfortunately, there are no literature reports on a single-crystal structure for any β -alkylglycosides [17] and many dry alkylglycosides are non-crystalline materials, which make the properties of the non-crystalline state interesting to study [17]. On the other hand, the crystal structures of some phospholipids have been determined by X-ray, for examples dilauroylphosphatidyl-ethanolamine (DLPE) [18, 19] and

dimiristoylphosphatidylcholine (DMPC) [20]. However, it was found that the lipid molecules in the crystal phase behave like lipids in a non-crystalline bilayer except for several important features such as the observation of gauche kinks in the L_β (gel phase) and L_α [21]. Noticeably, the hydrocarbon chain of the four understudied molecules is identical and only the configuration of the head group region is different from one molecule to another. This allows us to study the effects of the sugar head groups on bilayer related properties in a systematic manner.

In the current work, we have also taken advantage of some recent advancement in computer technology, especially in graphic processing unit (GPU), which has provided opportunities to perform complex simulation effectively, to enable longer simulation run and larger system size [22]. Current updates on simulation software like AMBER 12 [23] (for bio-molecular simulation) use GPU power to perform simulation by accommodating systems with hundreds to millions of particles [23, 24]. Additionally, an improved force-field for carbohydrates like GLYCAM_06d [25] is used to model and simulate glycolipids assembly systems to study structure and function relationships [26–28].

Methods

System description and simulation details

Each starting glycoside molecule (α/β -C8Gal and α/β -C8Glc) was built and geometry optimized using the HyperChem package [29]. The initial structure of each single bilayer of α/β -C8Gal and α/β -C8Glc was obtained by arranging a 10×10 array of 100 optimized lipids in the x and y plane, which constituted the first monolayer leaflet. The bilayer with the tail groups pointing to its center and the head groups facing the opposite direction was obtained using packmol [30]. GLYCAM_06d [25] and the *ff99* [31] force fields were used to assign the atom types, bond length, bond angle, dihedral angle, and partial charges for the carbohydrate head group and the tail group, respectively. The GLYCAM_06 contains all the parameters for sugar and lipids [25]. For carbohydrates, it has a single parameter set applicable to both α - and β -anomers and to all monosaccharide ring sizes and conformations [25]. The *ff99* force field is a derivative of the original Cornell et al. *ff94* force field [32], where improvements have been made in many torsional parameters. Such parameterization supports both additive and non-additive (polarizable) force fields [32]. The *ff99* force field has been extensively used for MD simulation of the biomolecular systems [26, 33, 34]. Additionally, alkyl chain carbon atoms on α/β -C8Gal and α/β -C8Glc were assigned a charge of zero implying non-ionic surfactant nature. The molecular dynamics (MD) simulation was performed on each system using AMBER12 software package [23, 24]. Prior to the actual molecular dynamics

run, the energy minimization using first the steepest descent (SD) algorithm followed by applying the adopted basis Newton-Raphson method, was performed to eliminate any unfavorable contacts and overlapping of atoms resulting from the model building procedure [23]. Pre-equilibration under the constant number of particles N , volume, V , and temperature, T , (NVT-ensemble) of the energy minimized structures was performed for 2 ns by increasing the temperature from 0 to 90 °C using the Andersen thermostat ($\tau_p=0.5$ ps) [35] with a 1 fs time step. Subsequently, the molecular dynamics simulation of the glycolipid lamellar system was carried out under the condition of constant number of particles N , pressure, p , and temperature, T (NpT-ensemble). Periodic boundary conditions were applied to the simulation box in all three coordinate directions (with x , y in the bilayer plane, and z normal to the bilayer) in cubic lattice geometry. The Berendsen pressure coupling method is normally used to simulate the bilayer system either anisotropically or semi-isotropically [36]. In the anisotropic case, the three unit-cell dimensions fluctuate independently, and the total pressure p remains constant at 1 bar, corresponding to an $Np_x p_y p_z T$ ensemble, unlike the semi-isotropic case, which gives an $Np_{NPL} T$ ensemble, where p_N and p_L are pressures along the normal and lateral to the bilayer respectively. In general, the two pressure coupling methods produce equilibrium properties, which cannot be differentiated statistically [14]. However the advantage of the semi-isotropic case is, the interface maintains a square, while in the anisotropic case the simulation box fluctuates independently in x and y directions [37]. Therefore, in our simulation we have used the semi-isotropic pressure coupling method, with a time constant 1 ps and a compressibility of 4.5×10^{-5} /bar. The simulation temperature was set at 363 K (or 90 °C) for all four glucosides.

Non-bonded interactions were truncated with a cut-off range of 9.0 Å and long-range electrostatic interactions were treated using the particle mesh Ewald summation method [38, 39]. The SHAKE algorithm was used to constrain covalent bonds involving hydrogen atoms [40]. The time step was 1 fs and the simulation's trajectories were saved once every 5 ps. The simulation was performed for a total duration of 200 ns dynamics. The equilibrium condition of the bilayer was monitored using two parameters: area per lipid and the local density profiles (LDPs). Block averages of the local density profiles (LDPs) over 20 ns were calculated for the entire 200 ns simulation. The LDPs show small fluctuation in the interface, but does not change significantly after 40 ns, so we assume 40 ns is sufficient for the system to reach its equilibrium and the bilayer properties are calculated from the last 160 ns. The area per lipid is very sensitive to the simulation details and is generally considered to be a reliable criterion for comparing and validating the simulation results [14]. Incidentally, these simulations were performed using the GPU-accelerated version of the *pmemd* simulation engine on

NVIDIA Tesla graphic card. A typical simulation performance for these systems on a normal PC-hardware is 18 ns/day, which is more than an order of magnitude higher than that of a typical CPU-based simulation [41].

Analysis

We have measured various structural and dynamical properties from the simulation. In order to monitor the stability of the bilayers, 20 ns block averages [14, 26] of the local density profiles (LDPs) were calculated up to 200 ns. Generally, the LDP was calculated along the bilayer normal, taking the center of the bilayer as the origin. This distribution function $g(z)$ was calculated from the number density, $\rho(x,y,z)$, given as:

$$N = \iiint \rho(x,y,z) dx dy dz, \quad (1)$$

where N is the total number of atoms. Along the z -direction, we defined $g(z)$ as:

$$g(z) = \Delta z \iint \rho(x,y,z) dx dy / N = \Delta z \rho(z) / N, \quad (2)$$

where A is the bilayer area, Δz is the bin size along the z -axis, and V is the volume. In addition, the convergence of the simulated system to its equilibrium state may be monitored through the time evolution of the surface area at the interface per lipid which is calculated by dividing the total area in the x and y directions of the bilayer by the total number of glycolipids (100) in a single bilayer leaflet [42]. Area per lipid is one of the parameters that can be used to determine how well equilibrated the simulated system is [43] because among the bulk quantities it gives a more detailed convergence perspective [44]. It was found that from the total 200 ns simulation run, the first 40 ns dynamics could be regarded as the equilibrium phase. Subsequently, for the analysis purposed, every 5 ps frame was archived from the last 160 ns dynamics. The conformational disorder of the hydrophobic chain is related to the state of the bilayer, where it is more disordered in a liquid-crystal than in a gel or a crystal phase [44]. Therefore the chain order parameter S_{CH} has been used to estimate the degree of ordering in the chain region. This is derived from a general 3×3 Saupe ordering tensor, S whose element, S_{ij} is,

$$S_{ij} = \frac{1}{2} \left(\overline{3 \cos \theta_i \cos \theta_j - \delta_{ij}} \right), \quad (3)$$

where θ_i is the angle between the i^{th} molecular axis and the bilayer normal, and the bar represents the time or ensemble averaged quantity [45]. The alkyl chain order parameter was defined according to van der Ploeg and Berendsen [46], where

the molecular axes for the n^{th} methylene group are defined by the H–H vector (x -axis), the bisectrix of the H–C_{*n*}–H angle (y -axis), and the vector C_{*n*–1} to C_{*n*+1} (z -axis). From the symmetry argument, the second order tensor S is diagonal and S_{zz} illustrates the chain order parameter. S_{zz} takes a value of unity if the average orientation is parallel to the bilayer normal (i.e., fully ordered), $-1/2$ if it is perpendicular to the normal, and zero if the system is completely disordered. S_{CH} is related to S_{CD} determine by the deuterium NMR experiment, where:

$$S_{CH} = S_{CD} = \frac{2}{3}S_{xx} + \frac{1}{3}S_{yy}, \quad (4)$$

where S_{xx} and S_{yy} are the order parameters in the x and y directions, respectively.

Inter- and intra-molecular hydrogen bond analysis was performed in each layer using the *ptraj* module in AMBER12, and CARNAL (AMBER7) respectively, by defining the O–O distance to be ≤ 3.5 Å and 4 Å and the cut-off angle of 120° from linearity. Since the results of both O–O distances are almost similar we show only the results of O–O distance ≤ 3.5 Å here. The tilt angle for the head group orientation was calculated based on the definition used by Rog et al. [47]. The vector representing sugar head group is defined from C8–O4 (see Fig. 2) and the orientation of the head group is defined by the angle between this vector and bilayer normal (along z -axis). In this study we chose the above vector definition for the sugar head group to compare the results obtained by others and subsequently discern the effect of chain length [48] and branching [47] on the sugar head stereochemistry. Furthermore, to examine the dynamic behavior of sugar molecules in the bilayer system, we computed the mean square displacement (MSD) of the translational diffusion for the sugars at the lipid surface using the *ptraj* module in AMBER. Generally, the translational mobility of lipids in the bilayer membrane model is considered to be two-dimensional. The lateral diffusion of the molecules was evaluated from the mean square displacement (MSD) of their center of mass in two-dimension, i.e., $\langle \Delta r_{xy}(t) \rangle$, where Δr_{xy} denotes the displacement of center of mass for a molecule.

Results and discussion

Local density profiles (LDPs)

The 20 ns block averages of the local density profiles for four systems (α/β -C8Gal and α/β -C8Glc) over the last 160 ns are given in Fig. 3. The LDPs show the bilayers do not break, even though there are minor differences between different block averages during the simulation. The expected micro-phase separation of the hydrophilic and the hydrophobic regions is demonstrated by the maximum and minimum density values along the bilayer normal in this figure. This implies that

throughout the simulation the structures are intact. The LDPs of the four systems (α/β -C8Gal and α/β -Glc) are qualitatively similar in general. However, for the four systems, their d -spacing are different, implying that these bilayers have slightly different packing arrangements, which eventually affect their melting points [7, 49]. The experimental bilayer spacing at 25 °C for β -C8Gal is 25.1 Å, while at 90 °C this value is 25.8 Å (Table 1), which is slightly less than the simulated value of 27.5 Å at 90 °C. Similarly, for β -C8Glc the simulated value of 27.5 Å is slightly more than the experimentally determined X-ray d -spacing of 25.6 Å and 25.3 Å at 70 °C and 105 °C, respectively [7]. Generally the present data for d -spacings are in accord with those from the X-ray measurements for these phases within less than 10 %. This percentage difference is not too dissimilar from those found in other simulation studies of disaccharides in thermotropic phase when compared with the experimental data [26, 50, 51]. In addition, it seems for β -C8Glc/C8Gal increasing the temperature does not change the thickness very much. Table 1 also shows that the bilayer spacings for α -anomers are smaller than those of the β -anomers, which imply the former pack more tightly compared to the latter. Comparing the d -spacing of the quartets (α/β -C8Gal and α/β -C8Glc) reveals that the anomeric effect is more dominant than the epimeric effect.

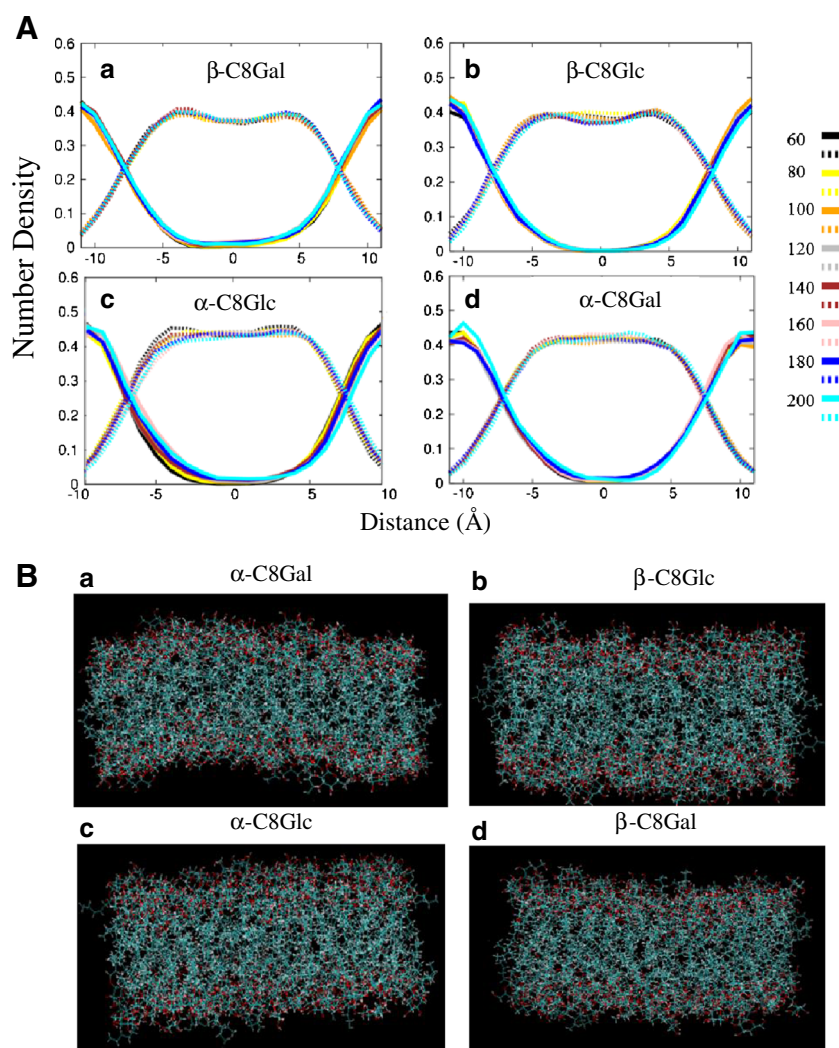
Area at the interface per sugar head

The average surface area at the interface per sugar head group over 160 ns dynamics runs for the four selected glycosides namely α/β -C8Gal and α/β -C8Glc, are given in Table 1. This data shows that the areas for α -C8Glc and α -C8Gal with the values of 36.0 and 35.1 Å² respectively are greater than those of β -C8Glc and β -C8Gal by 10–12 %. These results show the anomeric factor is important in controlling this property in the same manner as in the case of d -spacing. Thus, both thickness and interfacial area per head group are less sensitive to the C4 epimeric effect. According to the phase diagrams, both α/β -C8Glc and α -C8Gal are in the L_α phase. Therefore, chains within this phase are more fluid. In contrast, at this temperature β -C8Gal is in the L_C phase but very close to the transition into the L_α phase. Hence, it was observed that the β -C8Gal bilayer has the least area per head group (32.2 ± 0.4) Å². Our results show that α -anomers have higher surface area at the interface and lower densities than β -anomers.

Hydrogen bonds analysis

For a sugar-based surfactant system in a dry state, the sugar heads interact strongly with each other to stabilize the bilayer. This interaction originates mainly from the hydrogen bonds between sugar hydroxyl groups which makes sugar surfactants very fascinating in terms of their solid state behavior [56]. In addition, detailed sugar stereochemistry could

Fig. 3 (A) Local density profiles: averages over a block of 20 ns from 40 ns to 200 ns for (a) β -C8Gal, (b) β -C8Glc, (c) α -C8Glc, and (d) α -C8Gal. The solid lines are for head group and the dotted lines are for alkyl chain. Each colored line in the legend shows the LDPs of different 20 ns block averages spread over the 160 ns production stage. (B) Equilibrated bilayer structure for (a) α -C8Gal, (b) β -C8Glc, (c) α -C8Glc, and (d) β -C8Gal



generate hydrophobic or apolar surface on the sugar moiety giving its amphoteric character, which is important for molecular recognition [57, 58]. Glycolipid system has the ability to participate in hydrogen bonding as both donor and acceptors, unlike phosphatidylcholines, which can act only as an acceptor [47, 59]. Each sugar head group in the bilayer system can be involved in two types of hydrogen bonds: inter- and intra-molecular hydrogen bonds. The results of hydrogen bonds for

four sugar surfactants (α/β -C8Glc and α/β -C8Gal) are tabulated in Table 2. β -C8Gal has more affinity to be involved in both inter- (3.21) and intra-molecular (1.71) hydrogen bonds compared to β -C8Glc whose values are 3.06 and 1.12 respectively. In the former the hydroxyl group at C4 is oriented axially [7]. On the other hand, the inter-molecular hydrogen bond for α -C8Gal is 2.37 while that for α -C8Glc is 3.10. However, a reverse trend is observed for intra-molecular

Table 1 d -spacing for β -C8Gal in L_C phase, α -C8Gal and α/β -C8Glc in L_α phase and their average surface areas at the interface per lipid from 160 ns simulations and the corresponding X-ray experimental data

Lipid	Simulation at 90 °C		Experimental data from X-ray	
	d -spacing/Å	Area/head group(Å ²)	d -spacing/Å	Area/head group/Å ²
β -C8Gal	27.5±0.4 (L_C)	32.2±0.4	25.1/25.8 (at 25/90 °C)[7]	34.49 ^a
β -C8Glc	27.6±0.3 (L_α)	32.3±0.3	25.6/25.3 (at 70/105 °C)[7]	36.1 [53, 54]
α -C8Glc	24.4±0.2 (L_α)	36.0±0.3	23.3 (at 75 °C)[52]	39.1 [16]
α -C8Gal	25.4±0.3 (L_α)	35.1±0.4	NA	—

^a calculated from the data of ref. [55]

Table 2 Total number of hydrogen bonds per sugar for α -C8Glc, β -C8Glc, α -C8Gal, and β -C8Gal comprised of inter-molecular and intra-molecular hydrogen bonds

Mol/HB	β -C8Gal	α -C8Glc	β -C8Glc	α -C8Gal	Trend
Inter-mol	3.21	3.10	3.06	2.37	β -C8Gal > α -C8Glc > β -C8Glc > α -C8Gal
Intra-mol	1.71	1.31	1.12	1.71	α -C8Gal > β -C8Gal > α -C8Glc > β -C8Glc
Total	4.92	4.41	4.18	4.08	β -C8Gal > α -C8Glc > β -C8Glc > α -C8Gal
Exp. clearing point °C	127[7]	116[7]	107[7]	98[10]	β -C8Gal > α -C8Glc > β -C8Glc > α -C8Gal
Calc. clearing point °C	132	115	107	72	β -C8Gal > α -C8Glc > β -C8Glc > α -C8Gal
Exp. melting point °C	96[7]	69[7]	69[7]	40[10]	
From other literature					
Intra-layer [13]27(°C)	2.9	2.77	2.70	2.43	β -C8Gal > α -C8Glc > β -C8Glc > α -C8Gal
Inter-mol [47]70(°C)	1.63 ^a	–	1.28 ^a	–	DP-C8GALA > DP-GLUC
Inter-mol [27]	2.14 ^b	–	1.8 ^b	–	β -C8Gal > β -C8Glc

^a Calculation is in lyotropic phase, ^b Calculation is in micellar phase

hydrogen bonds with the values of 1.31 and 1.71 for α -C8Glc and α -C8Gal respectively. Table 2 also shows that, the trend for the total hydrogen bonds of the four compounds is the same as that of the inter-molecular hydrogen bonds, i.e., β -C8Gal > α -C8Glc > β -C8Glc > α -C8Gal.

This trend is also similar to the clearing temperatures of the four compounds, both from experimental and calculated based on the intermolecular hydrogen bond. In Table 2, the calculated clearing temperature assumes β -C8Glc is the reference compound. In the Supplementary T1, we have included all the calculated clearing temperatures, using different compounds as a reference. These predicted clearing temperatures are consistent with each other within less than 3 %, except when using α -C8Gal as a reference, where the difference is about 10 %. Thus, it supports the previous proposal that inter-molecular hydrogen bonds contribute to the thermal stability of the bilayer assembly [10].

Moreover, the axially orientated hydroxyl group at C4 makes α/β -C8Gal more capable of being involved in the intra-molecular hydrogen bonds than α/β -C8Glc. Incidentally, these results agree with those reported by Mosapour et al., [60] who had performed DFT calculations and analyzed them using atoms in molecules approach (AIM) and natural bond orbital analysis (NBO). The AIM results proved that for β -C8Glc there is one intra-molecular hydrogen bond (HO6...O4), while for β -C8Gal, there are two extra bonds (HO6...O4 and HO6...O3) [60]. In fact the inter-molecular hydrogen bond trend we observed here for the four glycosides agree with the same trend (intra-layer hydrogen bond) from the previous simulation [13]. Of course quantitatively, the detailed numbers differ since their systems were simulated at 300 K, for 5 ns simulation run. The total lipid-lipid hydrogen bonds for these glycosides are about 40–50 % higher than those of 1,2-di-*O*-palmitoyl-3-*O*- β -D-C8galactosyl-*sn*-glycerol (DP-C8GALA) and 1,2-di-*O*-palmitoyl-3-*O*- β -D-glucosyl-*sn*-glycerol (DP-GLUC) [47]. Lower values of lipid-lipid inter-

molecular hydrogen bonds for these glycosides are expected since the simulations were conducted in the lyotropic phase, where there was a variety of hydrogen bonds involving lipid-lipid, lipid-water, water-bridge, and H-bonded water [47]. However, the trend for hydrogen bonds (of DP-C8GALA versus DP-GLUC) agrees with the present results of galactosides versus glucosides. A similar pattern of dependency was also observed in the micellar (L_1) systems of for β -C8Gal and β -C8Glc, with the total number of inter head group hydrogen bonds at 2.14 and 1.8 respectively [27].

The role of polar interaction of the monosaccharide head group is important to stabilize the self-assembly. In theory, the maximum number of hydrogen bonds which a monosaccharide can make is 16, corresponding to six oxygen atoms able to accept two hydrogen bonds and four polar hydrogen atoms able to donate a hydrogen bond. Simulation result of the bilayer system shows the values are less than 16 and these are 4.92, 4.41, 4.18, and 4.08 for β -C8Gal, α -C8Glc, β -C8Glc, and α -C8Gal, respectively. Orientation constraint of hydroxyl groups and the steric effect in the bulk environment are some of the reasons, which cause the decrease of hydrogen bonding ability of the sugar head group [26]. It is interesting to calculate the distribution of these hydrogen bonds over the different OHs sites on the sugar moiety. Figure 4 shows the results of the individual donor and acceptor contributions to hydrogen bonding. A closer look into this in Fig. 4 reveals that the interaction scheme of inter-lipid hydrogen bonding are dominated by oxygen O2 and O6 in all four compounds (α/β -C8Gal and α/β -C8Glc), which suggests greater availability of O2 and O6 to accept inter-head group hydrogen bonds. The low interaction for O1 and O5 is expected based on the missing hydrogen donor ability due to the lack of a proton acceptor. In general O2 contributes almost 45 % more in hydrogen bonding compared to O3 in all four compounds, but the order and trend of hydrogen bond of the quartet on both sites are almost the same (see Fig. 4). Specifically, the

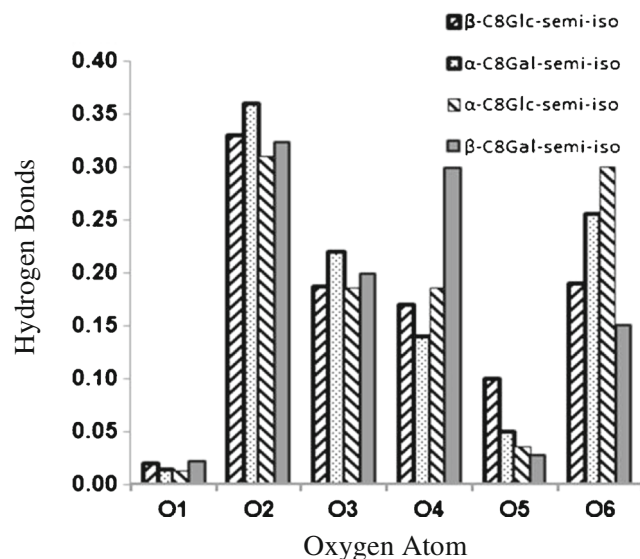


Fig. 4 Inter-molecular hydrogen bond distribution over different oxygen locations (see Fig. 2) for β -C8Glc, α -C8Gal, α -C8Glc, and β -C8Gal

trend for the hydrogen bond distribution on O2 and O3 of the four compounds is α -C8Gal > β -C8Gal > β -C8Glc > α -C8Glc. But this trend is slightly different for the O6 site, which is α -C8Glc > α -C8Gal > β -C8Glc > β -C8Gal. Thus, on O2 and O3, the epimeric effect is more dominant, while on O6 the anomeric effect is more dominant. The hydrogen bonding trend on the O4 site is β -C8Gal > α -C8Glc > β -C8Glc > α -C8Gal, which is similar to the overall trend for hydrogen bonding. Even though β -C8Gal and α -C8Glc are anomericly different, the hydrogen bonds on the O4 site of the former and the O6 site of the latter contribute nearly 80 % of the total hydrogen bonds. The axial orientation of OH on the O4 epimer in β -C8Gal causes the increase in the capacity of donor and acceptor of this compound. On the other hand, for α -C8Glc the exocyclic group at C6 position extends out to form a hydrogen bond with neighboring lipids. These hydrogen bond interactions may be attributed to the high clearing temperatures of 127°C and 116°C for β -C8Gal and α -C8Glc, respectively.

Head group orientation

Figure 5 shows the distribution of the angle between the C8–O4 vector and the bilayer normal [47]. From the non-Gaussian plots, we observe the population maxima occur at 28° and 36° for β -anomeric pairs, β -C8Gal and β -C8Glc respectively; whereas, for the α -anomeric pairs, α -C8Glc and α -C8Gal, these occur at 42° and 40° respectively. We notice that β -C8Gal, which is in the L_C phase, is tilting significantly less compared to the other isomers, which are in the fluid L_α . As expected, β -anomers are tilting less than α -anomers for the equatorially linked anomeric carbon to the glycosidic oxygen. The angle distribution profiles for β -C8Glc and β -C8Gal from

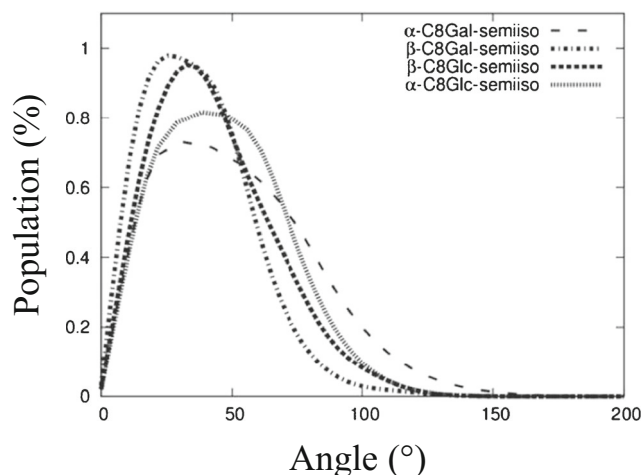


Fig. 5 Distribution of angles between C8–O4 vector and bilayer normal in α -C8Gal, β -C8Gal, β -C8Glc, and α -C8Glc bilayers

the current study are similar to those from the published work by Rog et al. [47], for β -anomers of DP-C8GALA and DP-GLUC with di-palmitic chains in L_α lyotropic phase. This similarity indicates that the orientation of sugar head group is not much affected by the branching and chain length. Moreover, in these cases the maxima occurred at about 38°, which is not too different from our measurement for the β -C8Glc (36°), in the anhydrous L_α , but is strikingly different from the dry L_C phase of β -C8Gal (28°).

Order parameter

Chain ordering in the bilayer is an interesting property used to determine the type of phase of the lipid assemblies [61]. Experimentally, deuterium nuclear magnetic resonance ($^2\text{H-NMR}$) measurement is used to determine the C–D bond order of the deuterated chain [62]. However, in a simulation, the order parameter is calculated using C–H bond and the Saupe ordering tensor, as in Eq. (3), and this is correlated with, the $-\langle S_{CD} \rangle$ [46]. Figure 6 shows the $-\langle S_{CD} \rangle$ as a function of the methylene carbon position [63, 64] for the four compounds. In general, the plot shows the bond (C–H) order parameter decreasing from C8 to C14 for the quartet α/β -C8Gal and α/β -C8Glc. The farther the position of the carbon from glycosidic bond, the less the order becomes; hence the increase in the flexibility of the chain. Van Buuren et al. also found the same diminishing chain ordering behavior for α/β -C10Glc in lyotropic systems [48]. It is interesting to note that the chain order parameters profiles (which are in the hydrophilic region) can be differentiated for the four compounds despite a diminutive difference in the head group stereochemistry. The two β compounds (β -C8Gal and β -C8Glc) have higher chain order parameter profiles compared to α compound (α -C8Gal and α -C8Glc). Except for β -C8Gal which is in the L_C phase, all other lipids are in the liquid crystalline, L_α phase. This leads to the

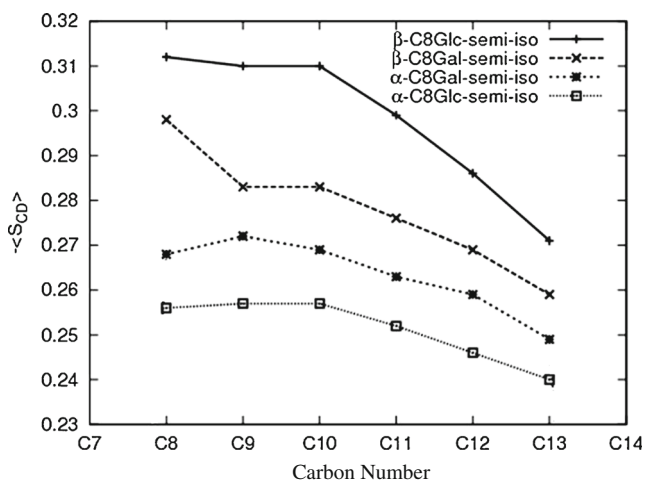


Fig. 6 The average bond order parameters of C–H along the chain, $-\langle S_{CD} \rangle$, for β -C8Gal (x), β -C8Glc (+), α -C8Gal (*), and α -C8Glc (□). Connecting lines drawn only as a guide. The error in these values is less than 4 %

expectation that the bond order parameter of β -C8Gal will be higher compared to that of the other three lipids. This is because in the L_{α} phase the chains are expected to be more disordered compared to those in the L_C phase. However, we observed a contradicting behavior, where β -C8Gal which is in the L_C phase, has a lower $-\langle S_{CD} \rangle$ profile than does β -C8Glc. This could be related to the higher hydrogen bonding interaction at C4 (see Fig. 4, O4) compared to those for the other lipids. The melting temperature of β -C8Gal is $96 \pm (5-8)^{\circ}\text{C}$ [7] which is very close to the simulated temperature 90°C . This observation may be justified from the thermal fluctuation viewpoint according to Sakya et al., [7] the high hydrogen bonding at the O4 position constrain the head group, but allows the chain to fluctuate more, thus lowering the order parameter in the L_C phase of β -C8Gal. Meanwhile, from Fig. 5 a higher degree of chain ordering is also related to a lower tilt angle of the chains. When the tilt angle is high, less chain packing is expected. Therefore, β -C8Glc and β -C8Gal with the smaller tilt angles have higher chain ordering.

Comparing the α/β anomers, α -anomers have lower order parameter compared to β -anomers. α -anomers give a bent molecular shape especially at the sugar head group to carbon chain and the arrangement in bilayer ordering of these molecules causes the alkyl chains to pack less densely. Similar results were observed for the *n*-decyl- α -D-glucopyranoside and *n*-decyl- β -D-glucopyranoside monolayers at the water-decane interface [48] which suggests that increased tilt of the α -glucose head groups leads to poorer packing of the decyl chains.

Lipid dynamics in anhydrous bilayer

The Einstein relation (also known as Einstein-Smoluchowski relation) of diffusion coefficient and mobility, for a typical system, where the particles motion is Brownian, should be

linear [65]. For this diffusion process, the mean square displacement (MSD) is linear in time with a constant slope representing the diffusion coefficient D . Deviation from this linearity indicates anomalous behavior, which can be categorized sub- or super-diffusion, and the MSD can be more generally defined as:

$$\langle \Delta r^2(t) \rangle = Dt^{\alpha} \quad \text{with } 0 < \alpha < 1 \quad (6)$$

$$\lg \langle \Delta r^2(t) \rangle = \lg D + \alpha \lg t, \quad (7)$$

where t denotes the time axis, and D is the diffusion coefficient which has the dimensionality of $\text{cm}^2/\text{sec}^{\alpha}$ [66]. The double logarithmic regression enables the determination of the power α of the diffusion law. When Einstein relation is satisfied α equals to one. On the other hand, when α is not equal to 1, the system experiences either a sub- ($\alpha < 1$) or super-diffusion ($\alpha > 1$). In nature, sub-diffusion is necessary for local interactions in cells [67] even though it slows down long-distance diffusional surface-bulk exchange [68]. For instance, the localization of objects such as chromosomes or membrane channels and the formation and dynamics of membrane domains, all depend on the magnitude of the exponent α [69].

In order to evaluate the lateral diffusion process in our bilayer systems, the double log MSD was calculated as a function of time (see Fig. 7), which displays the anomalous diffusion characteristics of the four lipid systems. This is based on Eq. (7), which describes the diffusion for both normal and anomalous systems [72]. This linear graph gives the exponent α and the diffusion coefficient D in Table 3. The observed sub-diffusive behavior of these lipids is reasonable and is attributed to the unique structural complexity of the sugar head group, consistent with those observed for phospholipids in the liquid disordered, liquid ordered, and gel

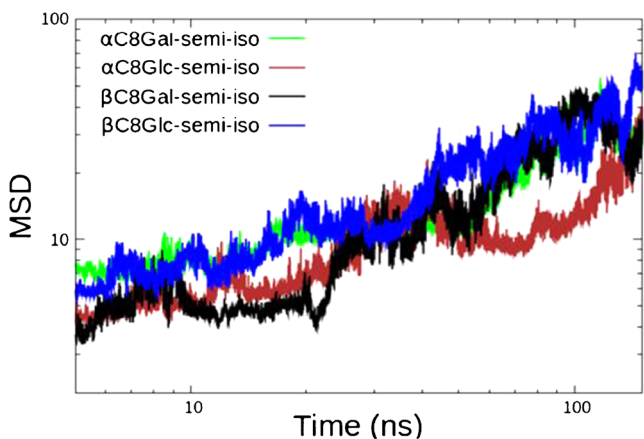


Fig. 7 Logarithmic scale of diffusion in xy direction for 160 ns for α/β -C8Gal and α/β -C8Glc

Table 3 The anomalous diffusion exponent, α and diffusion coefficient, D [$\times 10^{-8}$ m²/s] for α/β -C8Gal and α/β -C8Glc (40–200 ns) in dry state

Lipid	Exponent α	Calc. D [$\times 10^{-9}$ cm ² /s ^{α}]	Cis/trans-epimer/anomer
β -C8Gal	0.7 \pm (0.3 %)	9.0 \pm 0.3	Cis
β -C8Glc	0.6 \pm (0.2 %)	6.4 \pm 0.4	Trans
α -C8Gal	0.5 \pm (0.3 %)	6.2 \pm 0.3	Trans
α -C8Glc	0.5 \pm (0.4 %)	2.0 \pm 0.8	Cis
	Exp. D [$\times 10^{-8}$ cm ² /s]	Calc. D [$\times 10^{-8}$ cm ² /s]	
DPhPC	18.1 \pm 5.6[70, 71]	13.7 \pm 0.5[70]	In water
DPPD	20.7 \pm 2.8[70, 71]	35.3 \pm 0.6[70]	In water

phases [66]. From Table 3, we note also that the trans-epimer/anomer pair (β -C8Glc and α -C8Gal) in the L_α phase, have similar values of diffusion coefficients 6.4 and 6.2 ($\times 10^{-9}$ cm²/s ^{α}) respectively. The diffusion of the trans-epimer/anomer pair is similar to the gel phase of phospholipids bilayer membrane [66]. In contrast the cis-epimer/anomer pair has strikingly different values of diffusion coefficient, i.e., 9.0×10^{-9} cm²/s ^{α} for β -C8Gal (L_C phase), and 2.0×10^{-9} cm²/s ^{α} for α -C8Glc (L_α phase). These results may be understood from considering the thermal stability of these glycosides assembly with respect to their molecular structures. The thermal stability of amphiphilic liquid crystal is due to the hydrogen bond networks and the ability to store energy without disrupting the assembly. In the chain region, most of the energy will be stored in the vibrations of the alkyl chains [7]. Figure 8 shows the packing density and hydrogen bonding for α/β -anomeric pairs. The more linear shape of β -glycosides leads to a significantly more dense packing of the alkyl tails compared to the bent shape of the α -anomers. The former has less hydrophobic area for the chains to vibrate, and so they eventually push each other apart, hence greater diffusion

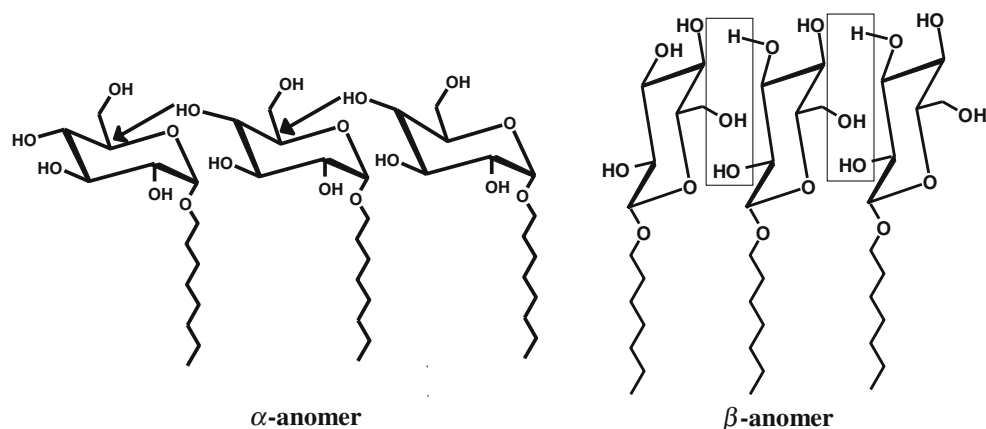
is expected. On the other hand, the chain groups of the α -anomers vibrate more due to the extra area in the chain region, and so the L_α phase is stable to higher temperatures [7].

In Table 3 we have included some experimental and simulation results of DPhPC and DPPC in the lyotropic phase for comparison. As expected, these lyotropic systems have larger diffusion coefficient compared to our dry systems.

Conclusions

Nowadays sugar-based amphiphilicities are among the most attractive classes of compounds to be studied both fundamentally and application-wise. The large diversity of sugar stereochemistry makes them an ideal prototype class of molecules for investigating the structure activity-function relationships. Here, we have applied fully atomistic MD simulations (200 ns) to investigate the stereochemical relationship of the epimeric/anomeric quartet liner glycolipids with the same octyl chain group, namely, α/β -octyl-galactosides and α/β -octyl-glucosides. Local density profile, inter- and intramolecular hydrogen bonds, average area at the interface per sugar, head group tilt angle, and chain order parameter are some of the properties which have been used to scrutinise the effect of subtle stereochemical changes of these systems.

The results show that, the anomeric stereochemistry or the axial/equatorial orientation of C1–O1 (α/β) is an important factor controlling the area and d -spacing of glycolipid bilayer systems in thermotropic phase, while the epimeric stereochemistry is secondary. Thus, thickness for β -C8Glc/C8Gal is larger than that for α -C8Glc/C8Gal. Meanwhile the area per lipid head group is higher for the α -compound than for the β -compound. In addition, the head group tilt angles are similar for those in the fluid L_α of about 36–42°, which is significantly larger than that for β -C8Gal in the L_C phase. Similarly, for the chain ordering property of the bilayer, the α -anomer was found to be less

Fig. 8 Packing density and hydrogen bonding for α/β -anomeric pairs

ordered compared to the β -anomer. Additionally, the assembly of sugar surfactant with α -anomer, in which the sugar head group bent to the hydrocarbon chain gave a slightly bent shaped molecular structure, while in bilayer arrangement the alkyl chains of these surfactants packed less densely.

On the other hand, the C4-epimeric (axial/equatorial) stereochemistry becomes dominant together with the anomeric one for the inter-molecular hydrogen bond. Thus, the trend in hydrogen bonding is β -C8Gal > α -C8Glc > β -C8Glc > α -C8Gal, which is in agreement with the previous studies of Hashim et al. [10] and Rog et al. [47] implying the axial orientation of the hydroxyl group on the C4 position in β -C8Gal increases the capacity of donor and acceptor of this compound. Likewise, the α -glucoside has a similar behavior. Therefore, these results support the proposal that when the hydroxyl group at the C4 carbon is cis with respect to the C1–O1 (i.e., β -C8Gal and α -C8Glc), greater bilayer stability is achieved compared to the case when these links are in a trans-configuration (i.e., β -C8Glc and α -C8Gal). The thermotropic bilayer of the four lipids studied here exhibited anomalous diffusion behaviors, where the observed trend for the diffusion coefficient for these compounds is (β -C8Gal > β -C8Glc > α -C8Gal > α -C8Glc). This trend shows that for a given epimer (gluco- or galacto-), β -anomer is more diffusive than the α -anomer. The latter has more space in the hydrophobic region, causing both chain vibration and chain disorganization to increase, but reducing the overall molecular diffusion, since thermal energy is dispensed more entropically for the chain region.

Acknowledgments The grants from the University of Malaya RG072-09AFR and the Ministry of Higher Education UM.C/625/1/HIR/MOHE/05 supported this project.

References

- Shallenberger RS (1982) Sugar chemistry. AVI, Westport
- Hashim R, Sugimura A, Minamikawa H, Heidelberg T (2012) Nature-like synthetic alkyl branched-chain glycolipids: a review on chemical structure and self-assembly properties. *Liq Cryst* 39(1):1–17
- Seddon JM, Ces O, Templar RH, Mannock DA, McElhaney RN (2003) Structure and phase behaviour of synthetic glycolipids. *Mol Cryst Liq Cryst* 402(1):77–84
- Vill V, Hashim R (2002) Carbohydrate liquid crystals: structure-property relationship of thermotropic and lyotropic glycolipids. *Curr Opin Colloid Interface Sci* 7(5):395–409
- Barón M (2001) Definitions of basic terms relating to low-molar-mass and polymer liquid crystals. *Pure Appl Chem* 73(5):845–895
- Lawrence MJ (1994) Surfactant systems: their use in drug delivery. *Chem Soc Rev* 23(6):417–424
- Sakya P, Seddon JM, Vill V (1997) Thermotropic and lyotropic phase behaviour of monoalkyl glycosides. *Liq Cryst* 23(3):409–424
- Balzer D, Luders H (2000) Nonionic surfactants: Alkyl polyglucosides. Dekker, New York
- Abel S, Dupradeau F-Y, Raman EP, MacKerell AD Jr, Marchi M (2011) Molecular simulations of dodecyl- β -maltoside micelles in water: Influence of the headgroup conformation and force field parameters. *J Phys Chem B* 115(3):487–499
- Hashim R, Mirzadeh SM, Heidelberg T, Minamikawa H, Yoshiaki T, Sugimura A (2011) A reevaluation of the epimeric and anomeric relationship of glucosides and galactosides in thermotropic liquid crystal self-assemblies. *Carbohydr Res* 346:2948–2956
- Boyd BJ, Drummond CJ, Krodskiewska I, Grieser F (2000) How chain length, headgroup polymerization, and anomeric configuration govern the thermotropic and lyotropic liquid crystalline phase behavior and the air-water interfacial adsorption of glucose-based surfactants. *Langmuir* 16(19):7359–7367
- Luzzati V (1968) X-ray diffraction studies of lipid-water systems. In: Chapman D (ed) *Biological membranes*, vol 1. Academic, London, pp 71–123
- Chong TT, Heidelberg T, Hashim R, Gary S (2007) Computer modelling and simulations of thermotropic and lyotropic alkyl glycoside bilayers. *Liq Cryst* 34(3):267–281
- Ane'zo C, de Vries AH, Holttje H-D, Tieleman DP, Marrink S-J (2003) Methodological issues in lipid bilayer simulations. *J Phys Chem B* 107(35):9424–9433
- Pedersen A, Henkelman G, Schiøtz J, Jónsson H (2009) Long time scale simulation of a grain boundary in copper. *New J Phys*. doi:10.1088/1367-2630/11/7/073034
- Kocherbitov V, Söderman O (2003) Phase diagram and physicochemical properties of the n-octyl α -D-glucoside/water system. *Phys Chem Chem Phys* 5(23):5262–5270
- Ericsson CA, Ericsson LC, Kocherbitov V, Söderman O, Ulvenlund S (2005) Thermotropic phase behaviour of long-chain alkylmaltosides. *Phys Chem Chem Phys* 7(15):2970–2977
- Elder M, Hitchcock P, Mason R, Shipley G (1977) A refinement analysis of the crystallography of the phospholipid, 1, 2-dilauroyl-DL-phosphatidylethanolamine, and some remarks on lipid-lipid and lipid-protein interactions. *Proc R Soc Lond A Mat* 354(1677):157–170
- Hitchcock PB, Mason R, Thomas KM, Shipley GG (1974) Structural chemistry of 1, 2 dilauroyl-DL-phosphatidylethanolamine: molecular conformation and intermolecular packing of phospholipids. *Proc Natl Acad Sci U S A* 71(8):3036–3040
- Pearson RH, Pascher I (1979) The molecular structure of lecithin dihydrate. *Nature* 281:499–501
- Damodaran KV, Merz KM Jr, Gaber BP (1992) Structure and dynamics of the ilauroylphosphatidylethanolamine lipid bilayer. *Biochemistry* 31(33):7656–7664
- van Meel JA, Arnold A, Frenkel D, Portegies Zwart SF, Belleman RG (2008) Harvesting graphics power for MD simulations. *Mol Simul* 34(3):259–266
- Case DA, Darden TA, Cheatham TEI, Simmerling CL, Wang J, Duke RE, Luo R, Walker RC, Zhang W, Merz KM, Roberts BP, Wang B, Hayik S, Roitberg A, Seabra G, Kolossvai I, Wong KF, Paesani F, Vanicek J, Liu J, Wu X, Brozell SR, Steinbrecher T, Gohlke H, Cai Q, Ye X, Wang J, Hsieh M-J, Cui G, Roe DR, Mathews DH, Seetin MG, Sagui C, Babin V, Luchko T, Gusarov S, Kovalenko A, Kollman PA (2012) AMBER 12. University of California, San Francisco
- Götz AW, Williamson MJ, Xu D, Poole D, Le Grand S, Walker RC (2012) Routine microsecond molecular dynamics simulations with AMBER on GPUs. 1. Generalized Born. *J Chem Theory Comput* 8(5):1542–1555
- Kirschner KN, Yongye AB, Tschampel SM, González-Outeiriño J, Daniels CR, Foley BL, Woods RJ (2008) GLYCAM06: a generalizable biomolecular force field. *Carbohydrates*. *J Comput Chem* 29(4): 622–655
- Manickam Achari V, Nguan HS, Heidelberg T, Bryce RA, Hashim R (2012) Molecular dynamics study of anhydrous lamellar structures of synthetic glycolipids: effects of chain branching and disaccharide headgroup. *J Phys Chem B* 106(38):11626–11634
- Chong TT, Hashim R, Bryce RA (2006) Molecular dynamics simulation of monoalkyl glycoside micelles in aqueous solution: influence of carbohydrate headgroup stereochemistry. *J Phys Chem B* 110(10): 4978–4984. doi:10.1021/jp056851g

28. Vishnyakov A, Widmalm G, Kowalewski J, Laaksonen A (1999) Molecular dynamics simulation of the α -D-Man p -(1 \rightarrow 3)- β -D-Glc p -OMe disaccharide in water and water/DMSO solution. *J Am Chem Soc* 121(23):5403–5412
29. HyperChem(TM) (2003) Hypercube, Inc., Gainesville, FL
30. Martínez L, Andrade R, Birgin EG, Martínez JM (2009) Packmol: A package for building initial configurations for molecular dynamics simulations. *J Comput Chem* 30(13):2157–2164
31. Hornak V, Abel R, Okur A, Strockbine B, Roitberg A, Simmerling C (2006) Comparison of multiple Amber force fields and development of improved protein backbone parameters. *Proteins Struct Funct Bioinform* 65(3):712–725
32. Case DA, Pearlman DA, Caldwell JW, Cheatham III TE, Wang J, Ross WS, Simmerling C, Darden T, Merz KM, Stanton RV (2002) University of California, San Francisco
33. Gong Z, Zhao Y, Xiao Y (2010) RNA stability under different combinations of Amber force fields and solvation models. *J Biomol Struct Dyn* 28(3):431–441
34. Spasic A, Serafini J, Mathews DH (2012) The Amber ff99 force field predicts relative free energy changes for RNA helix formation. *J Chem Theory Comput* 8(7):2497–2505
35. Andrea TA, Swope WC, Andersen HC (1983) The role of long ranged forces in determining the structure and properties of liquid water. *J Chem Phys* 79:4576
36. Berendsen HJC, Postma JPM, van Gunsteren WF, DiNola A, Haak JR (1984) Molecular dynamics with coupling to an external bath. *J Chem Phys* 81(8):3684–3690
37. Feller SE, Zhang Y, Pastor RW, Brooks BR (1995) Constant pressure molecular dynamics simulation: The Langevin piston method. *J Chem Phys* 103(11):4613–4621
38. Darden T, York D, Pedersen L (1993) Particle mesh Ewald: An $N \cdot \log(N)$ method for Ewald sums in large systems. *J Chem Phys* 98:10089
39. Essmann U, Perera L, Berkowitz ML, Darden T, Lee H, Pedersen LG (1995) A smooth particle mesh Ewald method. *J Chem Phys* 103(19):8577–8593
40. Miyamoto S, Kollman PA (1992) SETTLE: an analytical version of the SHAKE and RATTLE algorithm for rigid water models. *J Comput Chem* 13(8):952–962
41. Abou-Zied OK, Al-Lawatia N, Elstner M, Steinbrecher TB (2013) The binding of hydroxyquinoline probes to human serum albumin-combining molecular modeling and FRET spectroscopy to understand flexible ligand binding. *J Phys Chem B* 117(4):1062–1074
42. Petrache HI, Tu K, Nagle JF (1999) Analysis of simulated NMR order parameters for lipid bilayer structure determination. *Biophys J* 76(5):2479–2487
43. Shinoda W, Namiki N, Okazaki S (1997) Molecular dynamics study of a lipid bilayer: convergence, structure, and long-time dynamics. *J Chem Phys* 106:5731
44. Shinoda W, Mikami M, Baba T, Hato M (2003) Molecular dynamics study on the effect of chain branching on the physical properties of lipid bilayers: structural stability. *J Phys Chem B* 107(50):14030–14035
45. Losonczi JA, Andrec M, Fischer MW, Prestegard JH (1999) Order matrix analysis of residual dipolar couplings using singular value decomposition. *J Magn Reson* 138(2):334–342
46. van der Ploeg P, Berendsen HJC (1982) Molecular dynamics simulation of a bilayer membrane. *J Chem Phys* 76(6):3271–3276
47. Róg T, Vattulainen I, Bunker A, Karttunen M (2007) Glycolipid membranes through atomistic simulations: effect of glucose and galactose head groups on lipid bilayer properties. *J Phys Chem B* 111(34):10146–10154
48. van Buuren AR, Berendsen HJC (1994) Molecular dynamics simulations of carbohydrate-based surfactants in surfactant/water/oil systems. *Langmuir* 10(6):1703–1713
49. Nagle JF, Tristram-Nagle S (2000) Lipid bilayer structure. *Curr Opin Struct Biol* 10(4):474–480
50. Nguan HS, Heidelberg T, Hashim R, Tiddy GJT (2010) Quantitative analysis of the packing of alkyl glycosides: a comparison of linear and branched alkyl chains. *Liq Cryst* 37(9):1205–1213
51. Auvray X, Petipas C, Dupuy C, Louvet S, Anthore R, Rico-Lattes I, Lattes A (2001) Small-angle X-ray diffraction study of the thermotropic and lyotropic phases of five alkyl cyclic and acyclic disaccharides: Influence of the linkage between the hydrophilic and hydrophobic moieties. *Eur Phys J E* 4(4):489–504
52. Dorset DL (1990) Anomeric exchange and the structure of n -alkyl D-glucopyranosides. A study of binary phase behavior. *Carbohydr Res* 206(2):193–205
53. Nilsson F, Söderman O, Johansson I (1996) Physical-chemical properties of the n -octyl β -D-glucoside/water system. A phase diagram, self-diffusion NMR, and SAXS study. *Langmuir* 12(4):902–908
54. Kocherbitov V, Söderman O, Wadsö L (2002) Phase diagram and thermodynamics of the n -octyl β -D-glucoside/water system. *J Phys Chem B* 106(11):2910–2917
55. Seddon JM, Cevc G (1993) Lipid Polymorphism: Structure and Stability of Lyotropic Mesophases of Phospholipids. In: Cevc G (ed) *Phospholipids Handbook*. CRC, New York, pp 403–454
56. Ericsson CA, Ericsson LC, Ulvenlund S (2005) Solid-state phase behaviour of dodecylglycosides. *Carbohydr Res* 340(8):1529–1537
57. Jimenez-Barbero J, Junquera E, Martin-Pastor M, Sharma S, Vicent C, Penades S (1995) Molecular recognition of carbohydrates using a synthetic receptor. A model system to understand the stereoselectivity of a carbohydrate-carbohydrate interaction in water. *J Am Chem Soc* 117(45):11198–11204
58. Balasubramanian D, Raman B, Sundari CS (1993) Polysaccharides as amphiphiles. *J Am Chem Soc* 115(1):74–77
59. Pascher I (1976) Molecular arrangements in sphingolipids. Conformation and hydrogen bonding of ceramide and their implication on membrane stability and permeability. *Biochim Biophys Acta* 455(2):433–451
60. Kotena ZM, Behjatmanesh-Ardakani R, Hashim R, Achari VM (2013) Hydrogen bonds in galactopyranoside and glucopyranoside: a density functional theory study. *J Mol Model* 19(2):589–599
61. Mouritsen OG, Jørgensen K (1994) Dynamical order and disorder in lipid bilayers. *Chem Phys Lipids* 73(1):3–25
62. Marčelja S (1974) Chain ordering in liquid crystals: II. Structure of bilayer membranes. *Biochim Biophys Acta Biomembr* 367(2):165–176
63. Seelig J (1977) Deuterium magnetic resonance: theory and application to lipid membranes. *Q Rev Biophys* 10(3):353–418
64. Damodaran K, Merz KM Jr (1994) A comparison of DMPC-and DLPE-based lipid bilayers. *Biophys J* 66(4):1076–1087
65. Muddana HS, Gullapalli RR, Manias E, Butler PJ (2011) Atomistic simulation of lipid and DiI dynamics in membrane bilayers under tension. *Phys Chem Chem Phys* 13(4):1368–1378
66. Jeon JH, Monne HMS, Javanainen M, Metzler R (2012) Anomalous diffusion of phospholipids and cholesterol in a lipid bilayer and its origins. *Phys Rev Lett* 109(18):188103
67. Guigas G, Weiss M (2008) Sampling the cell with anomalous diffusion - the discovery of slowness. *Biophys J* 94(1):90–94
68. Lomholt MA, Zaid IM, Metzler R (2007) Subdiffusion and weak ergodicity breaking in the presence of a reactive boundary. *Phys Rev Lett* 98(20):200603
69. Bronstein I, Israel Y, Kepten E, Mai S, Shav-Tal Y, Barkai E, Garini Y (2009) Transient anomalous diffusion of telomeres in the nucleus of mammalian cells. *Phys Rev Lett* 103(1):018102
70. Shinoda W, Mikami M, Baba T, Hato M (2004) Dynamics of a highly branched lipid bilayer: a molecular dynamics study. *Chem Phys Lett* 390(1):35–40
71. Baba T, Minamikawa H, Hato M, Handa T (2001) Hydration and molecular motions in synthetic phytanyl-chained glycolipid vesicle membranes. *Biophys J* 81(6):3377–3386
72. Wu J, Berland KM (2008) Propagators and time-dependent diffusion coefficients for anomalous diffusion. *Biophys J* 95(4):2049–2052